Electrochimica Acta 54 (2009) 5531–5536

Contents lists available at ScienceDirect

Electrochimica Acta

journal homepage: www.elsevier.com/locate/electacta

Synthesis and characterization of carbon-coated $Li_{0.5}Ni_{0.25}TiOPO_4$ anode material

Kenza Maher[a], Kristina Edström[b], Ismael Saadoune[a,*], Torbjörn Gustafsson[a], Mohammed Mansori[a]

[a] University Cadi Ayyad, ECME, FST Marrakech, Av. A. Khattabi, BP549, Marrakech, Morocco
[b] Department of Materials Chemistry, Uppsala University, Box 538, SE-75121 Uppsala, Sweden

ARTICLE INFO

Article history:
Received 25 February 2009
Received in revised form 18 April 2009
Accepted 18 April 2009
Available online 3 May 2009

Keywords:
Lithium nickel oxyphosphate
Lithium ion batteries
Carbon coating
Raman spectroscopy

ABSTRACT

$Li_{0.5}Ni_{0.25}TiOPO_4$/C composite was synthesized by the co-precipitation method using polyethylene glycol as carbon source. X-ray diffraction study showed that the as-prepared material crystallizes in the monoclinic system (S.G. $P2_1/c$). This 3D structure exhibits an open framework favourable to intercalation reactions. The morphology and the microstructure characterisation was performed by scanning electron microscopy (SEM). Small particles (~1 μm) coated by carbon were observed. Raman study confirms the presence of carbon graphite in the $Li_{0.5}Ni_{0.25}TiOPO_4$/C composite. Cyclic voltammetry (CV) and charge–discharge galvanostatic cycling were used to characterize its electrochemical properties. The $Li_{0.5}Ni_{0.25}TiOPO_4$/C composite exhibits excellent electrochemical performances with good capacity retention for 50 cycles. Approximately 200 mAh/g could be reached at *C*, *C*/2, *C*/5 and *C*/20 rates in the 0.5–3 V potential range. These results clearly evidenced the positive effect of the carbon coating on the electrochemical properties of the studied phosphate.

1. Introduction

At the present time, considerable effort is applied for the development of new electric energy sources and improvement of the already known systems. In particular, great attention is focused on rechargeable Li-ion batteries. Many materials have been extensively studied as positive electrodes for lithium batteries, such as $LiCoO_2$ [1–3], $LiNiO_2$ [4,5] and $LiFePO_4$ [6–10]. $LiCoO_2$ shows a stable electrochemical performance over hundreds of cycles, but it delivers only half of the theoretically possible capacity. In addition, this material is expensive and not environmentally friendly. $LiNiO_2$ is an attractive cathode material because of its comparatively low cost, high theoretical capacity and environmental advantages compared to $LiCoO_2$ [11,12]. But it is extremely difficult to synthesize in reproducible conditions and the cycling behaviour is poor at high voltages.

Extensive research was also devoted to understanding and improving existing anode materials in today's lithium ion batteries. The most commonly used material is graphite [13]. Parallel to this, there is a great incentive to find new negative electrode materials that can store more lithium or function more safely than graphite. Among the developing material, the spinel $Li_4Ti_5O_{12}$ became an attractive alternative because it operates above the potential of lithiated graphite, thereby improving safety [14,15]. The experimental discharge capacity of this material is greater than 160 mAh/g.

Lithium transition metal phosphates are mainly used as positive electrode materials for Li-ion batteries. The existence of $M_n(PO_4)_y$ framework provides an excellent stability and long term cycling to this type of cathode in comparison to lithium transition metal oxides. Indeed, the oxygen–phosphorous bond is more covalent in nature than polar oxygen–metal bonds. Thus, no loss of oxygen occurs from the framework and the reactivity with the electrolyte is low [16]. Only one member of this class of materials, $LiFePO_4$, has become the answer to these requirements so far, also owing to other characteristics such as low cost, being environmentally benign and showing high safety. The main problem of $LiFePO_4$ lies in its poor rate capability, which is attributed to its low electronic conductivity and slow kinetics of lithium-ion diffusion trough the $LiFePO_4$–$FePO_4$ interfaces [17,18].

Several other lithium transition metal phosphates, including $LiTi_2(PO_4)_3$ [19], $Li_3Fe_2(PO_4)_3$ [20], $Li_2VOP_2O_7$ [21], $Ni_{0.5}TiOPO_4$ [22] and $Co_{0.5}TiOPO_4$ [23], have been intensively studied over the world. Concerning the two later oxyphosphates, their electrochemical features (especially the working potential) qualify these systems either as anodes for 5 V lithium ion batteries or as cathodes for applications requiring high energy density for medium voltages.

In the quest for other new framework materials based on the phosphate polyanion building block, we have investigated the electrochemical properties of $Li_{0.5}Ni_{0.25}TiOPO_4$ oxyphosphate. Single crystals of this material were firstly prepared by Manoun et al. [24]. The main disadvantage of this family of materials is their poor intrinsic electronic conductivity, which restricts their potential use

* Corresponding author. Tel.: +212 61 48 64 64; fax: +212 24 43 31 70.
E-mail address: saadoune1@yahoo.fr (I. Saadoune).

0013-4686/$ – see front matter © 2009 Elsevier Ltd. All rights reserved.
doi:10.1016/j.electacta.2009.04.053

as active material in Li-ion batteries. Fortunately, this problem could be solved by coating particles of the desired phosphate with carbon. Many different carbon sources are possible. Here, we use polyethylene glycol (PG) for the carbon-coating process.

In this paper, the carbon coated $Li_{0.5}Ni_{0.25}TiOPO_4$ has been synthesized by the co-precipitation method followed by the thermal treatment of the $Li_{0.5}Ni_{0.25}TiOPO_4$–PG mixture at 500 °C under a reducing atmosphere. In this way, PG is completely converted into electronically conductive carbon. The obtained composite was characterized by X-ray diffraction (XRD), scanning electron microscopy (SEM) and Raman spectroscopy. The electrochemical behaviour of the material was also studied. Note that in order to evidence the effect of additional carbon, we have prepared and studied the pure $Li_{0.5}Ni_{0.25}TiOPO_4$ within the same conditions.

2. Experimental

Microcrystalline $Li_{0.5}Ni_{0.25}TiO(PO_4)$ was prepared from a stoichiometric mixture between an aqueous solution of $LiNO_3$ (99%, Aldrich), $Ni(NO_3)_2{\cdot}6H_2O$ (99%, Aldrich), and $(NH_4)_2HPO_4$ (98%, Merck) with a solution of $TiCl_4$ (99% Aldrich) diluted in ethanol. A slow addition of titanium solution in the aqueous mixture with constant stirring, at room temperature, induces the formation of precipitates. After evaporation at 45 °C under vacuum, the resulting powder was progressively heated in air at 400 °C for 12 h to allow for the decomposition of the phosphate precursor and at 900 °C for 12 h to complete the synthesis of the desired oxyphosphate. A fine green powder was then obtained. One part of this obtained powder was dispersed with 10% in mass of polyethylene glycol (PG) powder in acetone. After evaporating the acetone, the mixture was heated to 500 °C for 12 h in a flow of CO/CO_2 gas (50:50).

The morphology of the samples was studied by scanning electron microscopy (SEM) using high resolution scanning electron microscopy (HRSEM LEO 1550).

The Raman spectra were collected at room temperature using a Renishaw 2000 spectrometer equipped with a 785 nm diode laser. Spectra were recorded in the 1900–100 cm^{-1} range.

The positive electrodes were prepared by mixing 75% active material, 10% super-P carbon powder and 15% PVDF (polyvinylideneflouride) binder in NMP (1-methyl-2-pyrrolidinone) solvent onto an aluminium foil. The coated aluminium was transferred into an argon-filled glove box (<1 ppm H_2O and O_2) and dried overnight in a vacuum oven at 120 °C. The cathode was assembled in a "coffee-bag" [25] (polymer laminated aluminium foil) type cell using a lithium foil as anode, an electrolyte of 1 M $LiClO_4$ in EC/DEC (Merck, battery grade and used as received) 2:1 by volume mixture and glass–wool separator. Charge–discharge tests were performed using a Digatron BTS 600 battery testing system with different rates and voltage cut-off positions at room temperature.

The cyclic voltammetry (CV) was carried out at 0.01 mV/s scanning rate in 0.5–4 V vs. Li/Li^+ potential range using VMP cycling system.

3. Results and discussion

3.1. Structural characterization

Fig. 1 shows the XRD patterns of the $Li_{0.5}Ni_{0.25}TiOPO_4$ sample (referred to as LNTP) and the $Li_{0.5}Ni_{0.25}TiOPO_4$/C composite (referred to as LNTP/C). The diffraction lines were indexed in the monoclinic system ($P2_1/c$ space group). However, two weak TiO_2 peaks were observed in the diffractograms. The Rietveld refinement of the XRD data in the hypothesis of the existence of two phases shows that the amount of the TiO_2 impurity was 4.7%.

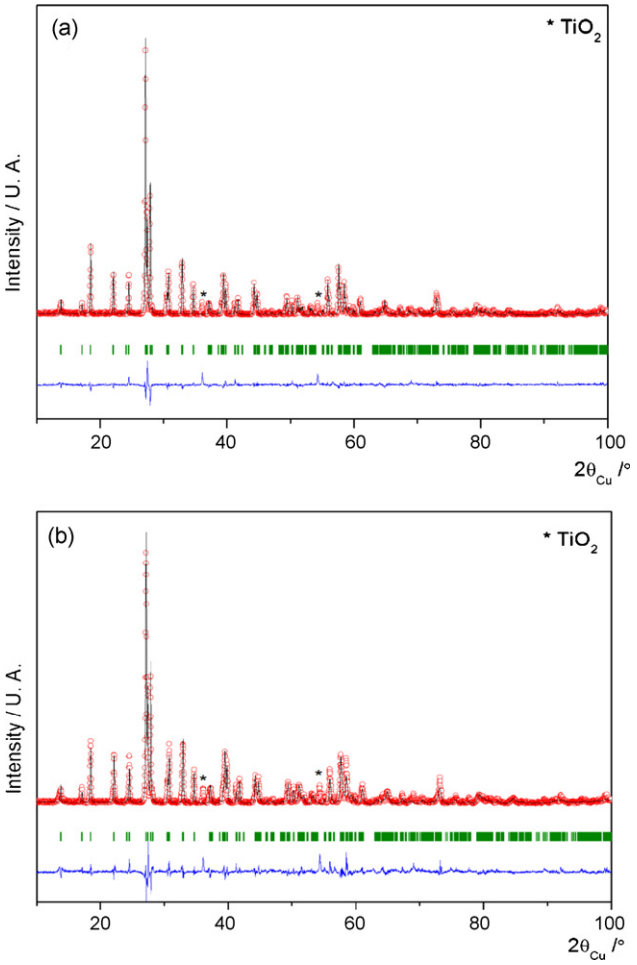

Fig. 1. Rietveld refinement of the XRD pattern of $Li_{0.5}Ni_{0.25}TiOPO_4$ (LNTP) (a) and $Li_{0.5}Ni_{0.25}TiOPO_4$/C (LNTP/C) composite (b). ((o) observed; (—) calculated; (|) Bragg position).

The XRD pattern of the LNTP powder shows narrower diffraction lines comparing to LNTP/C composite indicating better crystallinity with little difference between the observed and calculated patterns. Nevertheless, no significant difference in the unit cell parameters of the two studied materials has been evidenced. Note that no traces of carbon have been detected in the XRD pattern of the LNTP/C composite. This implies that the residual carbon is in an amorphous state. The structural data and details of the refinement, performed by using the Rietveld method, are summarized in Table 1. While the refined atomic parameters for $Li_{0.5}Ni_{0.25}TiOPO_4$ are given in Table 2. Note that the obtained atomic positions agree well with those obtained by Manoun et al. [24].

Fig. 2 shows the structure of LNTP. It can be described as three-dimensional networks of TiO_6 and NiO_6 octahedra and PO_4 tetrahedra within which Li^+ ions are located. Each TiO_6 octahedron shares one face with one NiO_6 octahedron, while NiO_6 octahedron shares corners with four PO_4 and two other corners with two TiO_6 octahedra. Lithium atoms fully occupy the site 2a, whereas nickel atoms occupy statistically half of the site 2b. As can be seen, the Ti^{4+} ions are isolated in the structure. This explains why the electronic conductivity (hopping mechanism) is very low in this phosphate.

3.2. Textural and morphology studies

Fig. 3a–d shows the SEM micrographs of the LNTP oxyphosphate and LNTP/C composite at different magnification. The SEM micrographs clearly show the difference in the microstructures.

Table 1
Structural data and X-ray Rietveld refinement parameters of $Li_{0.5}Ni_{0.25}TiOPO_4$ and $Li_{0.5}Ni_{0.25}TiOPO_4$/C.

	$Li_{0.5}Ni_{0.25}TiOPO_4$	$Li_{0.5}Ni_{0.25}TiOPO_4$/C
a (Å)	6.3924(4)	6.3925(1)
b (Å)	7.2535(1)	7.2538(8)
c (Å)	7.3673(3)	7.3677(6)
β (°)	90.1864(7)	90.1871(9)
Volume (Å^3); Z	341.604(4); 4	343.612(3); 4
Steps scan increment (2θ)(°)	0.02	0.02
2θ range (°)	10–100	10–100
Pseudo–Voigt function	$PV = \eta L + (1-\eta)G$	$PV = \eta L + (1-\eta)G$
Caglioti law parameters	$U = 0.0457(1)$; $V = -0.0310(2)$; $W = 0.0154(2)$	$U = 0.6123(4)$; $V = -0.3822(1)$; $W = 0.0642(3)$
System; space group	Monoclinic; $P2_1/c$	Monoclinic; $P2_1/c$
R_F	0.057	0.059
R_B	0.081	0.084
R_P	0.13	0.15
R_{wp}	0.17	0.18
cR_p	0.15	0.16
cR_{Wp}	0.20	0.21

The particles of the LNTP/C composite have a granular shape with an average particles size of 0.7 μm. Some of these particles seem to be interconnected. For the pure LNTP, the morphology is different. Some aggregates larger than 4 μm are present in this powder. This difference in morphology will play an important role for the electrochemical performances. Indeed, the small particle size and the interconnection between particles induced by the presence of carbon will enhance the electronic conductivity of the LNTP/C composite. Thus, an improvement of the electrochemical performance compared to that of LNTP is expected.

3.3. Raman spectroscopy

Raman analysis was used essentially to confirm the presence of the carbon coating layer in the LNTP/C composite.

Vibrational analysis for an isolated PO_4^{3-} anion with group T_d leads to four modes: A_1 (υ_1: $\upsilon_s(PO_4)$), E (υ_2: $\delta_s(PO_4)$) and $2T_2$ (υ_3: $\upsilon_{as}(PO_4)$ and υ_4: $\delta_{as}(PO_4)$). All of them are Raman active: $\Gamma = A_1 + E + 2T_2$

Fig. 4 gives a comparison of the Raman spectra of LNTP and LNTP/C. The high frequency part (900–1100 cm^{-1}) of these spectra corresponds to the stretching vibrations of the PO_4 tetrahedra in good agreement with results found for the homologous oxyphosphate $Ni_{0.5}TiOPO_4$ [26]. The peaks observed between 600 cm^{-1} and 300 cm^{-1} are attributed to the P–O bending vibrations, whereas those situated below 300 cm^{-1} are ascribed to the external modes. The intense band observed at approximately 760 cm^{-1} for the two studied compounds is attributed to the vibration of Ti–O bonds in the chains.

It should be noticed that two bands are observed between 1200 cm^{-1} and 1700 cm^{-1} for LNTP/C composite while they are absent in the pure $Li_{0.5}Ni_{0.25}TiOPO_4$ Raman spectrum. The existence of these two bands clearly indicates the presence of residual carbon in the LNTP/C composite.

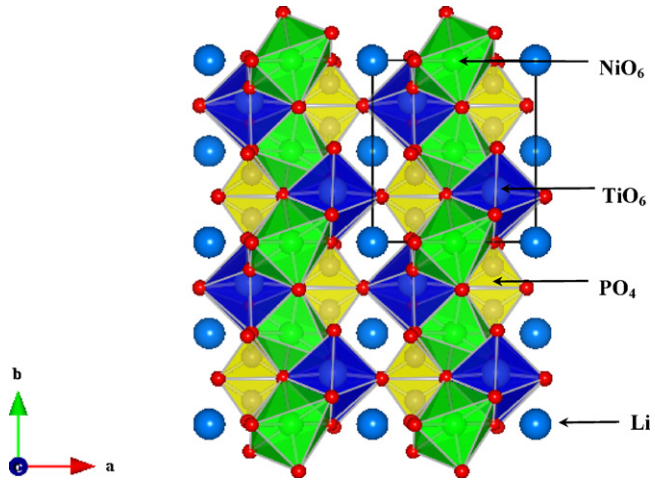

Fig. 2. The $Li_{0.5}Ni_{0.25}TiOPO_4$ structure.

3.4. Electrochemical properties

The cyclic voltametry (CV) curve of the LNTP/C composite for two cycles is shown in Fig. 5. The interesting feature is the difference between the first and second cycle. The first cathodic scan shows three reduction peaks. A major peak centred at 1.43 V corresponding to titanium reduction (from Ti^{4+} to Ti^{3+}), a medium at 1.24 V may be attributed to nickel reduction and a minor one, located at 0.80 V, corresponds to the reduction of the electrolyte components at the electrode surface leading to the well known solid electrolyte interfacial (SEI) film formation. In the subsequent cycles, the reduction and oxidation processes show only one cathodic and one anodic peaks centred at 1.4 V and 1.73 V, respectively which are attributed to the Ti^{4+}/Ti^{3+} redox couple. This irreversibility during the first discharge (Li insertion) is consistent with the results evidenced in the galvanostatic cycling experiment shown in Fig. 6. Indeed, three voltage plateaus are detected during the 1st discharge at approximately the same voltages mentioned above. Whereas during the subsequent charge (Li extraction), only one voltage plateau at ~1.72 V remains.

It should be noticed that the theoretical capacity of $Li_{0.5}Ni_{0.25}TiOPO_4$ electrode material is given by $Q_{calc.} = 150\Delta x$ mAh/g where Δx corresponds to the amount of the intercalated lithium-ions. Reduction of all active ions (Ni^{2+} and Ti^{4+}) involves the insertion of 1.5 lithium-ions corresponding

Table 2
Refined atomic parameters and their estimated standard deviations for $Li_{0.5}Ni_{0.25}TiOPO_4$.

Atom	Site	x	y	z	B (Å^2)	Occupancy
Li	2a	0.0000	0.0000	0.0000	0.38(3)	1.00
Ni	2b	0.5000	0.0000	0.0000	0.49(2)	0.50
Ti	4e	0.7563(6)	0.2196(4)	0.3337(5)	0.30(4)	1.00
P	4e	0.2608(1)	0.1299(1)	0.3738(2)	0.40(3)	1.00
O(1)	4e	0.7501(6)	0.1499(4)	0.1132(1)	0.29(2)	1.00
O(2)	4e	0.7414(3)	0.0028(1)	0.7941(4)	0.29(2)	1.00
O(3)	4e	0.2345(2)	0.4848(4)	0.0492(1)	0.29(2)	1.00
O(4)	4e	0.4522(2)	0.2594(2)	0.8639(2)	0.29(2)	1.00
O(5)	4e	0.9444(1)	0.7466(2)	0.1311(2)	0.29(2)	1.00

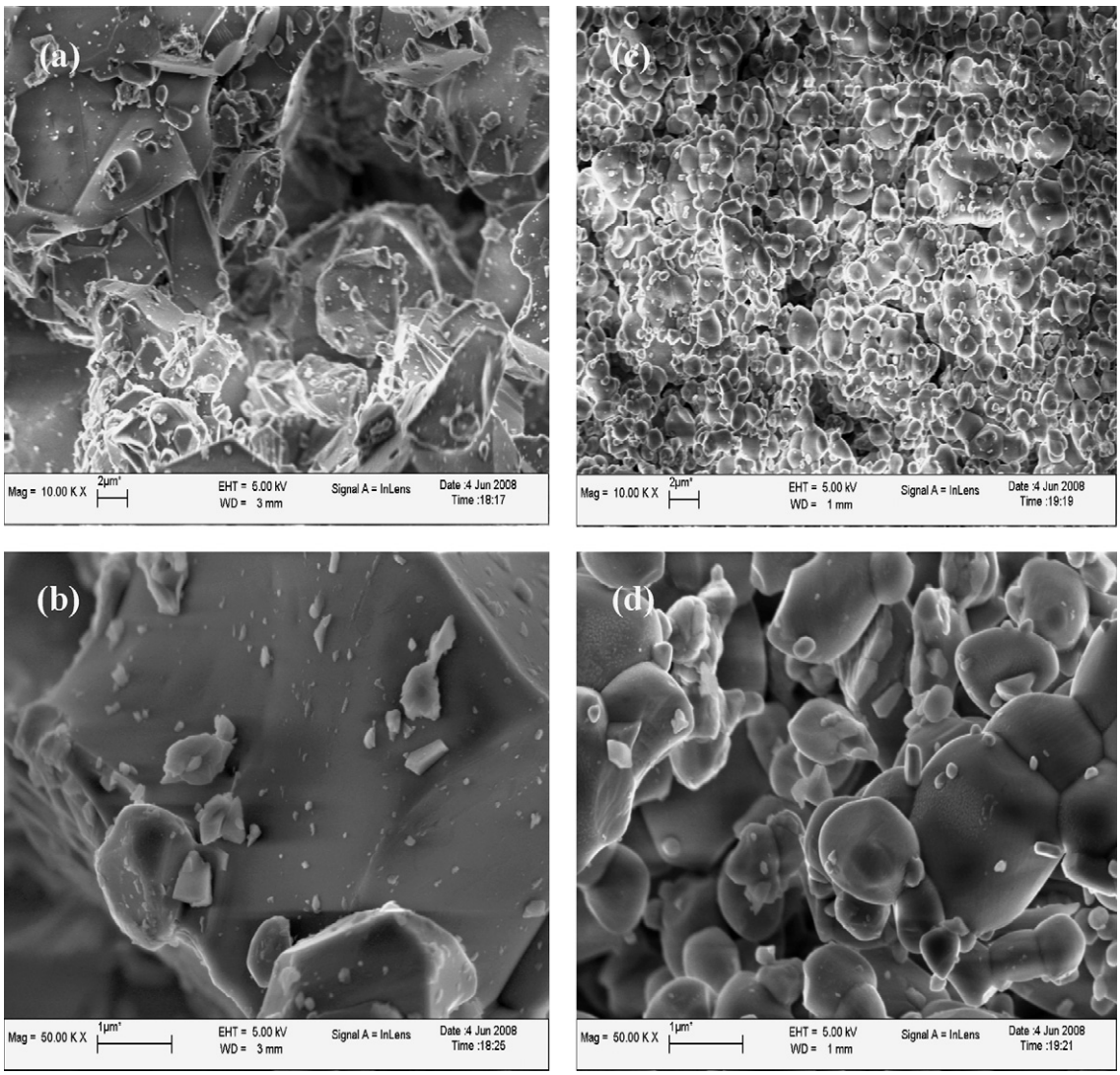

Fig. 3. SEM micrographs of LNTP oxyphosphate (a and b) and LNTP/C composite (c and d).

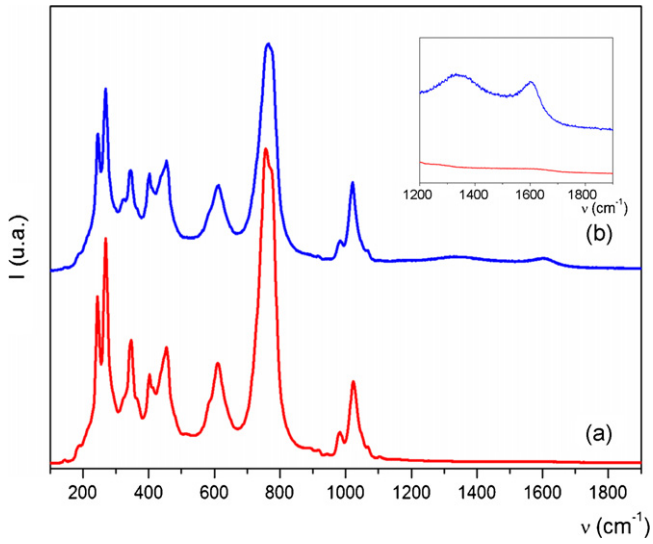

Fig. 4. Comparison between the Raman spectroscopy curves of LNTP oxyphosphate and LNTP/C composite.

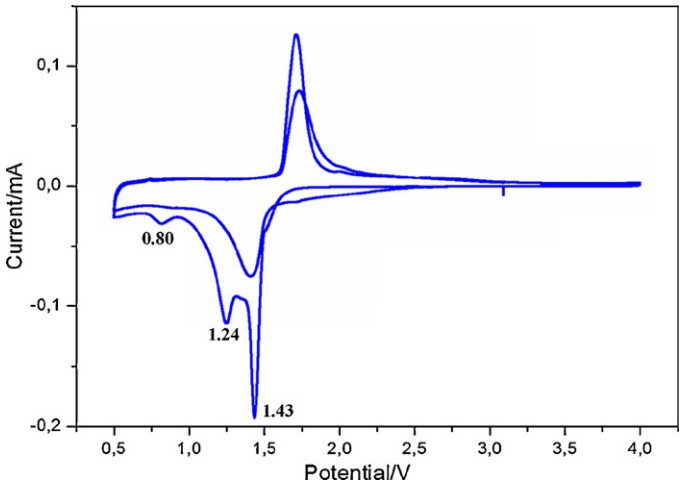

Fig. 5. The first two cyclic voltammograms of LNTP/C composite recorded in the 0.5–4 V voltage range. Scan rate: 0.01 mV/s.

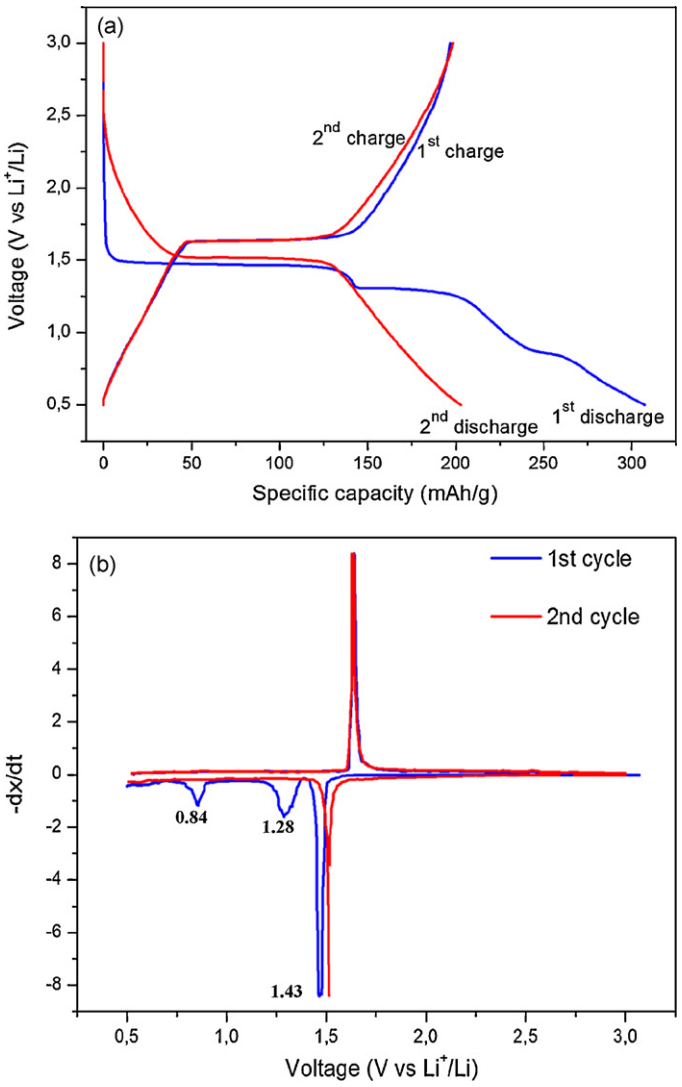

Fig. 6. First discharge/charge cycle and second discharge of the LNTP/C composite (a) and their derivative curve (b). Voltage range: 0.5–3 V; rate: *C*/20.

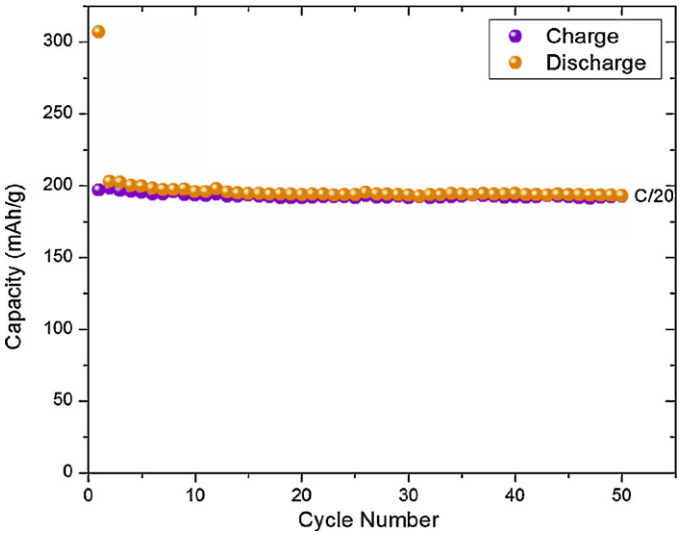

Fig. 7. Cycle performance of the LNTP/C composite at a *C*/20 rate in the 0.5–3 V potential range.

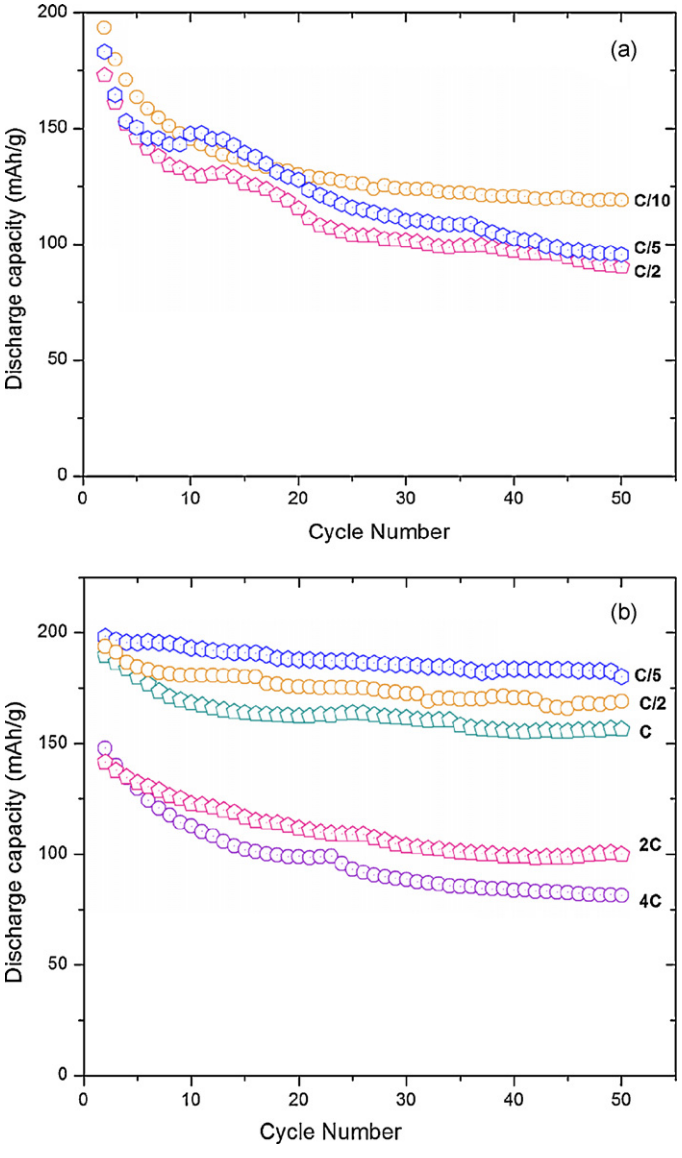

Fig. 8. The specific discharge capacities vs. cycle number of LNTP oxyphosphate (a) and LNTP/C composite (b).

to the Ti^{4+}/Ti^{3+} and Ni^{2+}/Ni redox couples. This implies that the theoretical capacity is equal to 225 mAh/g. This is an indication that the obtained experimental capacity during the first discharge (about 300 mAh/g) corresponds not only to the insertion of lithium-ions but also to the formation of the SEI interface. As shown in Fig. 6a, the plateau at ca 1.43 V corresponds to 147 mAh/g which corresponds to the reduction of one mole of Ti^{4+} ions ($\Delta x = 0.98$). During the subsequent cycles, the capacity remains constant and approximately equal to 200 mAh/g. This implies that the main active redox couple during $Li//Li_{0.5}Ni_{0.25}TiOPO_4$ electrochemical cell cycling is Ti^{4+}/Ti^{3+}. The excess experimental capacity during cycling could be associated to the Ni^{2+}/Ni redox couple.

In order to examine the preliminary life performance of LNTP/C composite, 50 charge/discharge cycles were carried out at low-rate. Fig. 7 shows the charge/discharge curves of the Li//LNTP/C electrochemical cell cycled between 0.5 V and 3 V at a *C*/20 rate. The first discharge capacity was 307 mAh/g. On charge, the capacity decreased to 200 mAh/g losing about one third of its discharge capacity. This capacity loss is probably due to the above mentioned irreversible electrochemical processes during the first discharge. During the following cycles, good reversible capacity retention and better cycleability were obtained.

Fig. 8a–b shows the results of rate capability tests performed at different rates starting from *C*/5 to 4*C* for LNTP/C composite and at *C*/10, *C*/5 and *C*/2 for the pure LNTP, in the voltage range 0.5–3 V. LNTP/C exhibited significantly better electrochemical performance with a specific capacity of 198 mAh/g at *C*/5. The discharge capacity loss is less than 15% after 50 cycles.

The 1st discharge capacity decreases from 195 mAh/g, 190 mAh/g, 141 mAh/g and 148 mAh/g for *C*/2, 1*C*, 2*C* and 4*C* rates to 169 mAh/g, 156 mAh/g, 100 mAh/g and 81 mAh/g at the 50th cycle. Thus, the excellent capacity retention obtained for *C*/5 rate has been maintained by the Li//LNTP/C cells upon progressive cycling at the *C*/2 and 1*C* regimes.

In contrast, the capacity of the pure $Li_{0.5}Ni_{0.25}TiOPO_4$ decreased continuously with further cycling at different rates. The discharge capacity was 193 mAh/g in the 2nd cycle but faded to 119 mAh/g after 50 cycles at the low regime *C*/10. This behaviour indicates that the rate capability of $Li_{0.5}Ni_{0.25}TiOPO_4$ was strongly enhanced by the presence of the residual carbon. It also confirms the negative effect of the low intrinsic electronic conductivity of phosphates on their electrochemical performance.

3.5. Conclusion

The carbon coated $Li_{0.5}Ni_{0.25}TiOPO_4$ was successfully prepared by using polyethylene glycol as carbon source, under a reducing atmosphere. Rietveld refinement of the X-ray diffraction patterns shows that this oxyphosphate exhibits a monoclinic symmetry (S.G. $P2_1/c$). The structure consists of a three-dimensional framework formed by $[TiO_6]$ and $[NiO_6]$ octahedra interconnected by $[PO_4]$ tetrahedral. Many vacancies exist within the structure, making it able to be a host material in the lithium batteries. The presence of carbon in the LNTP/C composite was detected only by Raman spectroscopy. SEM pictures show different particle shapes of LNTP/C comparing to the pure oxyphosphate. Carbon coated $Li_{0.5}Ni_{0.25}TiOPO_4$ exhibits smaller particles interconnected by carbon. Thus, excellent electrochemical performances were obtained for LNTP/C composite even at fast regime. An irreversible capacity was observed during the first discharge which was attributed to the formation of SEI film and Ni^{2+} reduction. During the subsequent cycles, the Ti^{4+}/Ti^{3+} redox couple is active together with the Ni^{2+}/Ni redox couple during the electrochemical cycling. The capacity retention ranges from 92% to 82% at *C*/5, *C*/2 and 1*C* rates even after 50 cycles. These performances are much higher than those obtained for the uncoated $Li_{0.5}Ni_{0.25}TiOPO_4$.

The low cycling potential (~1.7 V) and the good capacity retention during cycling are favourable to consider this oxyphosphate rather as a candidate for the negative electrode.

Acknowledgements

The authors gratefully acknowledge the financial support of the Swedish Research Council (VR MENA program), the Swedish Energy Agency and the Swedish Hybrid Vehicle Centre. Miss Maher Kenza thanks the CNRST-MESFCRS (Morocco) for the financial support.

References

[1] K. Mittzushima, P.C. Jones, P.J. Wiseman, J.B. Goodenough, Mater. Res. Bull. 15 (1980) 783.
[2] J.R. Dahn, U. von Sacken, C.A. Michal, Solid State Ionics 44 (1990) 265.
[3] K. Ozawa, Solid State Ionics 69 (1994) 212.
[4] C. Delmas, M. Ménétrier, L. Croguennec, I. Saadoune, A. Rougier, C. Pouillerie, G. Prado, M. Grüne, L. Fournès, Electrochim. Acta 45 (1999) 243.
[5] T. Ohzuku, A. Ueda, Solid State Ionics 201 (1994) 69.
[6] A.K. Padhi, K.S. Nanjundaswamy, J.B. Goodenough, J. Electrochem. Soc. 144 (1997) 1188.
[7] A.S. Andersson, J.O. Thomas, B. Kalska, L. Häggström, Electrochem. Solid-State Lett. 3 (2000) 66.
[8] A. Yamada, S.C. Chung, K. Hinokuma, J. Electrochem. Soc. 148 (2001) A224.
[9] S. Okada, S. Sawa, M. Egashira, J.I. Yamaki, M. Tabushi, J. Power Sources 97–98 (2001) 430.
[10] D.D. MacNeil, Z. Lu, Z. Chen, J.R. Dahn, J. Power Sources 108 (2002) 8.
[11] B.J. Neudecker, R.A. Zhur, B.S. Kwak, J.B. Bates, J. Electrochem. Soc. 145 (1998) 4148.
[12] C. Delmas, Mater. Sci. Eng. B 3 (1989) 97.
[13] J.R. Dahn, A.K. Sleigh, H. Shi, B.M. Way, W.J. Weydanz, J.N. Reimers, Q. Zhong, U. von Sacken, New materials developments and perspectives, in: G. Pistoia (Ed.), Lithium Batteries, Elsevier, Amsterdam, 1994.
[14] J. Shu, Electrochim. Acta 54 (2009) 2869.
[15] H. Kitoura, A. Hayashi, K. Tadanaga, M. Tatsumisago, J. Power Sources 189 (2009) 145.
[16] A.S. Andersson, J.O. Thomas, J. Power Sources 97–98 (2001) 498.
[17] H. Huang, T. Faulkner, J. Barker, M.Y. Saidi, J. Power Sources 189 (2009) 748.
[18] K. Zaghib, K. Striebel, A. Guefi, J. Shim, M. Armand, M. Gauthier, Electrochim. Acta 50 (2004) 263.
[19] C. Delmas, A. Nadiri, J.L. Soubeyroux, Solid State Ionics 28–30 (1988) 419.
[20] K.S. Nanjundaswamy, A.K. Padhi, J.B. Goodenough, S. Okada, H. Ohtsuka, H. Arai, J. Yamaki, Solid State Ionics 92 (1996) 1.
[21] M. Satya Kishore, V. Pralong, V. Caignaert, U.V. Varadaraju, B. Raveau, Solid State Sci. 10 (2008) 1285.
[22] I. Belharouak, K. Amine, Electrochem. Commun. 7 (2005) 648.
[23] R. Essehli, B. El Bali, H. Ehrenberg, I. Svoboda, N. Bramnik, H. Fuess, Mater. Res. Bull. 44 (2009) 817.
[24] B. Manoun, A. El Jazouli, P. Gravereau, J.P. Chaminade, F. Bourée, Powder Diff. 17 (2002) 290.
[25] T. Gustafsson, J.O. Thomas, R. Koksbang, G.C. Farrington, Electrochim. Acta 37 (1992) 1639.
[26] P. Gravereau, J.P. Chaminade, B. Manoun, S. Krimi, A. El Jazouli, Powder Diff. 14 (1) (1999) 10.